New Hamiltonian and Cooper pair's origin of both pseudogap and colossal magnetoresistance in manganites

Fu-sui Liu

Department of Physics, Beijing University, Beijing 100871, China
E-mail: fsliu@pku.edu.cn

Abstract

Based on the fifteen similarities of structures of lattice, electron, and strong correlation Hamiltonian between CMR (colossal magnetoresistance) manganites and the high-T_c cuprates, this paper concludes that the Hamiltonian of the high-T_c cuprates and CMR manganites are the same. Based on uniform and quantitative explanations for thirty seven experimental facts, this paper concludes that both the pseudogap and CMR of manganites are caused completely by formation of Cooper pairs, consisting of two oxygen $2p\sigma$ holes in MnO_2 plane. This paper gives some applications of CMR manganites, and predicts that 90% and 80% in applications of superconductors and semiconductors will be substituted by CMR manganites, respectively, in future 30 years.

1. Introduction

The manganites known as colossal magnetoresistance (CMR) manganese oxides continue to attract considerable attention due to the presence of CMR and pseudogap [1-21]. The pseudogap of manganites was observed for the first time by Dessau *et al.* in 1998. CMR had been observed in the fifties of the last century. Although there were more than fifteen proposed mechanisms on the pseudogap and CMR, no one mechanism can uniformly and quantitatively explain both the pseudogap and CMR, and no one mechanism connects with Cooper pair. CMR and pseudogap have not yet haven widely accepted mechanism. Theory falls behind experiment very far, is still in model stage, phenomenological, and has some obvious mistakes. Let me give you an example on the situation of theoretical studies.

A widely used models of manganites are one- or two-orbital, in which just one or two orbitals of $3de_g$ are considered, respectively (Eqs. (5.7) and (5.11) in Ref. [9]). However, experiments have observed that the itinerant carriers in manganites are doped oxygen $2p\sigma$ holes rather than $3de_g$ electrons [13]. However, at present, the common theoretical view is [9]: "However, adding the oxygen orbitals to the electronic models complicates enormously the theoretical studies, which are already quite difficult even with only Mn sites." It is obvious that the present any theories cannot correctly explain the observed facts on the pseudogap and CMR because both these are directly connect with carriers, and the carriers are 2p holes other than 3d electrons.

The goals in this paper are: (i). To point out fifteen similarities between CMR manganites and the high-T_c cuprates in aspects of lattice, electronic, and Hamiltonian; (ii). To prove the Cooper pair's origin of both pseudogap

and CMR of manganites by uniform explanations for the thirty seven key experimental facts; (iii). To give some applications of CMR manganites at room temperature; (iv). To emphasize the advantages of CMR manganites over superconductors and semiconductors.

2. The fifteen similarities between CMR manganites and high-T_c cuprates

The basic building block of manganites is the MnO_6 octahedron [7]. These octahedrons share their in-plane oxygen atoms, forming two dimensional MnO_2 planes, and in this plane, many effects occur [7]. The Fermi surface in MnO_2 plane has nesting structure [2]. The present angle-resolved photoemission studies of $(La_{1-z}Pr_z)_{2-2x}Sr_{1+2x}Mn_2O_7$ with x = 0.4 and z = 0.1; 0.4 along with density functional theory calculations and x-ray scattering data show that: (i). The bilayer splitting in the ferromagnetic metallic phase of these materials is small, if not completely absent; (ii). The charge carriers are therefore confined to a single MnO_2 plane, which in turn results in a strongly nested Fermi surface; (iii). At the same time, the spectral function displays clear signatures of an electronic ordering instability. The increase of the corresponding interaction strength with z and its magnitude of $\approx$ 400 meV, make a coupling to bare phonons highly unlikely. Instead it is concluded that the nematic electronic order strongly influences the charge carrier dynamics and causes the electronic confinement in these bilayer manganites [21]. The Mn^{3+} and Mn^{4+} ions are local spins $S = 2$ and $S = 3/2$, respectively [9]. Therefore, in both lattice and electronic structures the manganites and high-Tc cuprates are the same [11].

For the CuO_2 plane of the high-T_c cuprates, the strong correlated Hamil-

tonian is [21,11]

$$H = t_\circ \sum_{i,\alpha,s} (d_{is}^+ p_{\alpha s} + h.c) + U_d \sum_i n_{di\uparrow} n_{di\downarrow} + U_p \sum_\alpha n_{p\alpha\uparrow} n_{p\alpha\downarrow}$$
$$+ V_\circ \sum_{i,\alpha} n_{di} n_{p\alpha} + \epsilon_d \sum_i n_{di} + \epsilon_p \sum_\alpha n_{p\alpha}, \qquad (2.1)$$

where d_{is}^+ and $p_{\alpha s}^+$ create holes on the Cu:d and O:p orbits at sites i and α with spin $s = 1/2$, respectively, n_{di} $(n_{p\alpha})$ is the number operator of d (p) holes, $n_{di} \equiv n_{di\uparrow} + n_{di\downarrow}$, $n_{p\alpha} \equiv n_{p\alpha\uparrow} + n_{p\alpha\downarrow}$, $-t_\circ$ is the hopping integral for the holes between adjacent Cu:d and O:p orbits, and U_p, U_d, and $V_\circ$ are intra- and interatomic Coulomb repulsion on O:p orbits, Cu:d orbits, and between both orbits, respectively. The site index with an alphabetic letter stands for Cu site and that with a Greek letter stands for the O site in the CuO_2 plane. We use x to stand for the hole number in one unit cell of Cu lattice in the CuO_2 plane. At half-filling, $x = 0$, there exists one e_g hole per Cu site, i.e., Cu^{2+}; and for $x > 0$ extra holes go into O:p orbits and Cu^{2+} is stable under doping. If we take that the local spins are 2 or 3/2, then Eq. (2.1) becomes the strong correlated Hamiltonian of the MnO_2 planes.

By treating the first term as a perturbation, Ref. [21] derived an effective Hamiltonian, Ref. [11] made simplification, and the last form is

$$H = -\sum_{i\alpha\beta s} T_{\alpha\beta} p_{\alpha s}^+ p_{\beta s} + J_K \sum_{i\alpha\beta ss'} \widehat{\mathbf{S}}_i \cdot \overrightarrow{\sigma}_{ss'} p_{\alpha s}^+ p_{\beta s'} + J \sum_{ij(i<j)} \widehat{\mathbf{S}}_i \cdot \widehat{\mathbf{S}}_j$$
$$+ H_{hole-phonon} + H_{hole-hole}$$
$$\equiv H_{Kinetic} + H_{Kondo} + H_{Heisenberg} + H_{hole-phonon} + H_{hole-hole}, \qquad (2.1)'$$

where the summation over α and β stands for the oxygen sites around i-th Mn^{3+} site with local spin $S = 2$; $p_{\alpha s}$ annihilates $O_{p\sigma}$ hole with spin s=1/2 at site α; $\widehat{\mathbf{S}}_i$ is the local spin operator of Mn^{3+} at site i; $\overrightarrow{\sigma}$ is Pauli matrix vector; and i and j are the nearest neighbors. $J > 0$ and $J < 0$ are AFM and FM Heisenberg Hamiltonian, respectively.

The Hamiltonian in Eq. (2.1)′ has many different points in comparison with the until now widely accepted Hamiltonian of manganites in Eqs. (5.6-11) of Ref. [9]):

(i). $-T_{\alpha\beta} \simeq t_\circ$ is the hopping integral between Mn^{3+} and O^{2-} rather than the hopping integral t between Mn^{3+} and Mn^{3+} [9];

(ii). Our Kondo term represents the interaction between the $2p$ hole and the local spins ($S \equiv 2$) of Mn^{3+} ion, rather than that between the electron of $3de_g$ and Mn^{4+} ion with $S = 3/2$. The serious mistakes of the previous Hamiltonian are: (a). In the previous Kondo Hamiltonian, J_K is substituted by Huns energy J_H. We think that this is a conceptual mistake. According to the basic definition, the Hund energy can only exist in an isolated atom or ion. However, the $3de_g$ electron in the Kondo term of one- nd two-orbital Hamiltonians is itinerant; (b). By the way, if we do not take our Kondo coupling constant $J_K(\approx 0.2)$ eV, and instead take Hund energy $J_H(\approx 2)$ eV, then our numerical simulations give, for example, the pseudogap is 1000 eV! (c). In Eq. (2.1)′, the Kondo Hamiltonian is derived rather than a phenomenological term (Refer to Eq. (5.1) of Ref. [9]);

(iii). The third term in Eq. (2.1)′ can be both FM ($J < 0$) and AFM ($J > 0$) rather than only AFM and a phenomenological term (Refer to Eq. (5.3) of Ref. [9]); If the manganites are in FM state rather than in AFM state, then the "Double-Exchange" and other FM interactions give this term;

(iv). The $H_{hole-phonon}$ represents the coupling between $2p$ hole (rather than $3de_g$ electron [9]) and the Jahn-Teller distortions of the local MnO_6 octahedron. This term should also include the breathing model; (v). $H_{hole-hole}$ represents the Coulomb interaction among the $2p$ holes rather than the $3de_g$ electrons.

It is easy to observe that the first three terms in Eq. (2.1)′ can cause an

indirect exchange interaction between two itinerant $2p$ holes in MnO_2 plane. This indirect interaction is mediated by two nearest neighbour FM or AFM coupling local spins at sites of Mn^{3+} or Mn^{4+} ions (See Fig. 3.2 in Ref. [11].). This indirect interaction is called two local spin-mediated interaction (TLSMI), and can cause Cooper pairing in both macroscopic superconductive state and pseudogap state, in which the systems do not have macroscopic superconductivity in the MnO_2 plane or the high-T_c cuprates [11].

The first three terms of Hamiltonians in Eq. $(2.1)'$ and Eq. (3.5) in Ref. [11] are the same. Using more than fifty pages, Ref. [11] derives the mathematical expression of TLSMI, obtains the solutions of BCS gap equation, gives the numerical program to calculate pseudogap and pairing probability of individual carrier. We can use all the formulas in Ref. [11], and just in the stage of numerical calculations substitute the values of related parameters of the high-T_c cuprates by the values of CMR manganites. The values of parameters of CMR are given in section 3. For $S = 2$ Ref. [11] Can give

$$TLSMI = -A\frac{272(cos\theta)^2 N'' JJ_K^2}{T^2 + B272 \times 64(cos\theta)^2 JJ_K^2/\{1 + C20J_K^2\}},$$
$$(2.2) \ (See \ (3.74) \ and \ many \ related \ formulas \ of \ [11])$$

where A, B, , C are constants, N'' is determined by the size of the cluster with magnetic order, for long-range magnetic order the size of cluster is infinite, N'' has maximum value 2, the minimum value is $N'' = 1$, and θ is the angle between two nearest neighbour Mn ions in FM coupling case (In AFM case $\theta \equiv 0$.) [11].

The pseudogap functions are of p- and d-wave symmetry for FM and AFM, and give in Eqs. (3.67-68) and Eq. (3.66), respectively [11].

Table 1 lists the fifteen similarities as a summary of this section.

3. Values of parameters of manganites

In this section you can see that the values of related parameters for CMR manganites and high-T_c cuprates are nearly equal. We have to use the values of related parameters of CMR manganites for exact comparisons of data with numerical results. All the values of parameters of CMR manganites can be found in the present available references. Eqs. (5.26-5.35) of Ref. [11] show that J_K is a function of $U_d, \Delta_{eff}, V_\circ$. $\Delta_{eff} = 1.8\ eV$ and $U_d = 6.8\ eV$ [13]. The hopping integral t between Mn^{3+} and Mn^{3+} is 0.2 - 1 eV [9]. We take $t_\circ = 0.5$ eV. Of course, if the on-site Coulomb repulsion energy $U_d = 6.8$ eV, then the Coulomb repulsion energy between Mn^{3+} and Cu^{2-}, $V_\circ$, will much less than 6.8 eV. Referring to the CuO_2 plane of high-T_c cuprates, we take $V_\circ = 1.0$ eV [11]. $J = 0.05$ eV [9]. Bandwidth is 1.8 eV [2]. (for reference: the effective mass of itinerant hole is $m_{eff} = 0.3m_e$, m_e is the electron mass, average free path is 1.44 nm, Fermi velocity is 0.38c, $U_d = 7\ eV$ [7]. $m_{eff} = 3.3m_e$, the average free path is 2.5 nm [2].)

4. Numerical results and explanations for experiments

4.1. Pseudogap

(1). Fig. 1 shows the experimental data of the pseudogap versus temperature for $La_{0.625}Ca_{0.375}MnO_3$.

Explanation: Our theoretical cure in Fig. 1 can quantitatively explain the data well.

Please look at the point (6) of this subsection for more explanations on the pseudogap.

(2). Fig. 2 shows the experimental data of the pseudogap versus temper-

ature for $La_{2-2x}Sr_{1+2x}Mn_2O_7$ with $x = 0.4$.

Explanation: Our theoretical cure in Fig. 2 can quantitatively explain the data well.

(3). Refs. [16,1] reported that for the sample $La_{2-2x}Sr_{1+2x}Mn_2O_7$ with $x = 0.4$ at $T > 126$ K the pseudogap is observed in the entire Fermi surface, and there is no zero pseudogap anisotropy.

Explanation: The theory in section 2 indicates that in FM state the pseudogap is of p-wave symmetry. Our numerical simulations show that for $La_{2-2x}Sr_{1+2x}Mn_2O_7$ with $x = 0.4$ in FM state the minimum and maximum pseudogap is along the $Mn - O$ bond and $45°$ away from $Mn - O$ bond directions, respectively. The ratio is $\Delta(Mn - O)/\Delta(45°) = 0.358/0.626 \neq 0$.

(4). Ref. [2] observed that the pseudogap of $La_{2-2x}Sr_{1+2x}Mn_2O_7$ with $x = 0.4$ is of d-wave symmetry at 20 K other than p-wave symmetry.

Explanation: There is phase transition from pure FM to coexistence of FM and AFM at $15 < T < 40$ K in the MnO_2 plane [9]. Our numerical simulations show that in the same values of parameters the d-wave is much easier to occur than the p-wave. This theoretical result can explain the observed d-wave (other than p-wave) pseudogap at $T = 20$ K.

(5). Many different types of magnetic systems can have pseudogap [11,6].

Explanation: Many quite different types of magnetic systems can have, in principle, the same Hamiltonian structure as the first three terms of Eq. $(2.1)'$ [21,1]. So long as a system has the Hamiltonian liking to the first three terms in Eq. (2.1) and there are some appropriate values of parameters, then this system will have the pseudogap certainly.

(6). Ref. [3] pointed out the present representative viewpoints on the pseudogap: "The hole doped colossal magnetoresistive (CMR) manganites [1] have attracted much attention in the past two decades for their intriguing

physics and application potential. The Zener double exchange [2] mechanism that explained the CMR behavior was found to be insufficient [3] and this led to a more elaborate theory by Millis, Shraiman, and Mueller (MSM) incorporating Jahn-Teller (JT) interaction [4]. As evidenced by a number of experiments, like Hall effect [5], transport [6], X- ray spectroscopy [7], scattering [8], and isotope effect [9], the JT small polarons (SP) [10] seem to be responsible for the activated resistivity in the paramagnetic insulating (PI) phase of manganites. Several experiments such as neutron scattering [8], optical conductivity [11], photoemission [12], and tunneling [21, 28], have also shown signatures of polarons in the ferromagnetic metallic (FM) phase; although these signatures are weaker, at least the structural ones [7, 8], than those in PI phase. Moreover, the optical Drude weight [11] and recent angle resolved photoemission spectroscopy (ARPES) [13] observation of a quasi-particle peak at EF indicate the presence of free carriers as well in the FM phase. Besides MSM theory [4], which finds a transformation of SP into delocalized carriers at TIM, a number of other models have also been proposed in the recent past. Emin [14] suggested that these delocalized carriers are large polarons with larger spatial extent of lattice deformation. Alexandrov and co-workers [15] advocate the splitting of singlet bipolarons at high temperatures into SP below TIM. Both these models propose only polaronic states in the FM phase. Another simple model, put forward by Ramakrishna and coworkers [16], accounts for the free carriers by having delocalized band states together with localized polarons. In addition, this model proposes a coherent SP state at low temperatures to account for small magnitude of resistivity. Therefore, both the theory and experiment point towards some kind of polaron softening or delocalization with the onset of the ferromagnetic order. However, the detailed physics of the FM phase seems far from understood. In

particular, the role of charge carriers, i.e. whether they are free or polaronic, in the FM state is not yet clear."

According to our numerical calculations in point (1), the pseudogap comes from the formation of Cooper pair, which consists of two free $O_{p\sigma}$ holes in the MnO_2 plane, and is independent completely of any kinds of polarons or any kinds of polarizations. At least at present, there is only our theory on the pseudogap can uniformly and quantitative explain the temperature dependence of the pseudogap at regions of above and below the Curie temperature. The viewpoint of Cooper pair on the pseudogap in the high-T_c cuprates has been verified by many observations and theories such as Refs. [22,11].

4.2. CMR

(1). In cases of both zero [15] and non-zero magnetic field [17] there are curves of magnetization versus temperature. In both cases the intervals between Curie temperature and saturating magnetization temperature are equal to the intervals between temperatures of high and low resistivity, respectively.

Explanation: The stronger the magnetic field or the stronger the magnetization is, the larger the factor $(cos\theta)^2$ in pairing potential TLSMI is. According to Landau criterion, the motion of Cooper pairs in pseudogap states is free although might be random [11,6]. The motion of Cooper pairs in the high-T_c cuprates has been verified [23]. Similar to the high-Tc cuprates [11,23,6], we refer CMR completely to the formation to Cooper pairs in the pseudogap state as well. Therefore, when we get larger number of Coop pairs, we get larger (negative) CMR.

(2). The data on the temperature dependence of CMR in single crystal $La_{1.2}Sr_{1.8}Mn_2O_7$ at different magnetic fields are reported by Refs. [14,15,9,8], which is shown in Fig. 3.

Explanation: In our calculations for the temperature dependence of CMR at 0 and 5 T, we naturally use the expression of resistivity

$$\rho_{ab} = \rho_0 Q(T) + \rho_1[1 - Q(T)], \qquad (4.1)$$

where $Q(T)$ represents the probability of one individual carrier to become one carrier of a Cooper pair, ρ_0 and ρ_1 represent residual resistivity and resistivity without Cooper pairs, respectively. Due to that we study CMR in $La_{1.2}Sr_{1.8}Mn_2O_7$, we neglect the small temperature dependence of rho_1. Refs. [11,6] have given the formula of $Q(T)$ (See Eq. (2.405) in Ref. [11]. According to Eq. (2.2), our numerical calculations need the experimental magnetization curves at H = 0, 5 T, which are given by Refs. [14-16].The better fitting between the data and our numerical result in Fig. 3 indicates that CMR is really completely caused by the formation of Cooper pairs in $La_{1.2}Sr_{1.8}Mn_2O_7$.

(3). The experiments found that the necessary condition occurring CMR is that the CMR manganites are in FM state [8,9].

Explanation: In FM state, the more stronger the applied field is $\Rightarrow$ the more stronger the FM order is $\Rightarrow$ the stronger the magnetization is $\Rightarrow$ the stronger the pairing potential TLSMI in Eq. (2.2) is $\Rightarrow$ the larger the number of Cooper pairs is $\Rightarrow$ the larger the (negative) CMR is.

(4). The magnitude of CMR is a linear function of square of magnetization around Curie temperature, where the magnetization is small [16].

Explanation: Eq. (2.2) indicates that the Cooper pairing potential is a function of square of magnetization, $\propto (cos\theta)^2$. The first order approximation of Taylor expansion in $\propto (cos\theta)^2$ is proportional to $\propto (cos\theta)^2$. The number of Cooper pairs should be dependent on TLSMI (Refer to Eq. (2.405) in Ref. [11].), and, thus, CMR is dependent on $\propto (cos\theta)^2$ linearly.

11

(5). The data in Fig. 3 show that all the interplane resistivities are equal approximately to the inplane resistivities plus about 39 Ωcm, correspondingly.

Explanation: The Cooper pairs are formed only in the MnO_2 plane. However, the Cooper pairs can tunnel from one MnO_2 plane to another nearest neighbor MnO_2 plane. The tunnel process is of resistance, and does not be sensitive to temperature. Thus, we obtain $\rho_c = \rho_{ab} + 39 \ \Omega cm$, where 39 Ωcm is the tunneling resistivity.

(6). The experimental data of resistivity versus temperature at different pressures from 1 atm to 6.0 GPa in sample $La_{0.33}Ca_{0.67}MnO_3$ show that the pressure causes CMR as well as magnetic field [18]. The variations of lattice constants a and b in the MnO_2 plane are: a=5.4610 and 5.4043, b=5.4750 and 5.4324 $\overset{\circ}{A}$ for 1 atm and 5.87 GPa, respectively [17].

Explanations: The larger the pressure is $\Rightarrow$ the shorter the lattice constant is $\Rightarrow$ the larger the value of J in Eq. (2.2) is [18] $\Rightarrow$ the larger the value of TLSMI is $\Rightarrow$ the larger the number of Cooper pairs $\Rightarrow$ the less the resistivity is.

(7). For $La_{0.625}Ca_{0.375}MnO_3$ $\rho(T = T_{M-I} = 120 \ K)/\rho(T = 100 \ K) = 30$ at a definite band width, and if the band width reduces, then $\rho(T = T_{M-I} = 240 \ K)/\rho(T = 100 \ K) = 1000$ [3]. Ref. [15] observed the effect of band width on resistivity as well.

Explanation: Our numerical calculations for $La_{1.2}Sr_{1.8}Mn_2O_7$ are as follows. $\rho(T = 126 \ K)/\rho(T = 100 \ K) = 18, 25, 31$ for band width $W = 1.8, 1.5, 1.2$ eV, respectively.

(8). CMR can occur in thallium manganite pyrochlores ($Tl_2^{3+}Mn_2^{4+}O_7$) without double-exchange [12].

Explanation: Our paring potential of Cooper pair, TLSMI, in Eq. (2.2) is completely independent of the double-exchange.

(9). Ref. [12] concluded clearly from experimental facts: "Thus, thallium manganite pyrochlores ($Tl_2^{3+}Mn_2^{4+}O_7$) has neither mixed valence for a double exchange-magnetic interaction nor a Jahn-Teller cation such as Mn^{3+}, which both are known to play an essence role in CMR perovskite materials."

Explanation: Although our new Hamiltonian in Eq. (2.2) can contain Jahn-Teller interaction, in all the above numerical calculations, which give the quantitative explanations for both the pseudogap and CMR, we do not consider the Jahn-Teller term. This fact points out that Jahn-Teller effect for the pseudogap and CMR is not important.

(10). The data for epitaxial film and polycrystalline (3, 14, 24 μm average grain size) of $LaCaMnO$ are that the small grain size leads to (i). High resistivity; (ii). Small CMR [13].

Explanation: (i). The conduction occurs in MnO_2 plane. Therefore, the less the grain's size is, the larger the tunneling resistivity between two grain's MnO_2 planes is; (ii). Eq. (2.2) indicates the Cooper pairing potential TLSMI is proportional to N''. The less the grain's size is $\Rightarrow$ the less the value of N'' is $\Rightarrow$ the less the value of $N'' \Rightarrow$ the less the TLSMI is $\Rightarrow$ the less the number of Cooper pairs $\Rightarrow$ the less the CMR is.

(11). There are two types of CMR [12,9]. The first type of CMR is given by Fig. 1.6. Another example of the first type is $Pr_{0.7}Sr_{0.05}Ca_{0.25}MnO_3$, for which a jump of resistivity of about five orders of magnitude at $T_{max} = 85$ K, which is shown in Figs. 1a and 1b in page 44 of Ref. [12], and can be explained by the reason for fact 6.

The second type of CMR is given by Figs. 2a and 2b in page 46 of Ref. [12] for $Pr_{0.5}Sr_{0.5}MnO_3$. Its resistivity reaches minimum at 140 K, and with decreasing temperature goes up [12,9].

Explanation: The phase diagram in Fig. 2b shows that at 140 K $Pr_{0.5}Sr_{0.5}MnO_3$

13

has a phase transition from FM metal to AFM insulator.

(12). Ref. [19] found that at $T < T_{Curie}$ and at zero or nonzero voltages there are emergent reversible giant electroresistances in spatially confined $La_{0.325}Pr_{0.3}Ca_{0.375}MnO_3$ wires with width, length, and thickness of 10 μm, 50 μm, and 90 nm, respectively. Micro-patterning is considered to be a promising way to analyze phase-separated manganites. A reentrant of charge-ordering insulating state (COI) at the metalCinsulator temperature $T_p = 91$ $K(< T_{Curie})$ is observed in some wire samples, and at $T < T_p$ a giant resistance change of over 90% driven by electric field is achieved by suppression of this COI state. Or, equivalently speaking, by applying electric field, the reentrant COI state is suppressed and finally diminished. This electric field suppression of the COI state leads to giant resistance decrease.

Explanation: Although the authors have proposed explanations for their observations. This paper proposes a possible other explanation from our theory of formation of Cooper pairs.

(i). The Fig. 2 of Ref. [19] shows that three samples, film, wire I, and wire II, have the nearly same residual resistivity. This fact indicates that all quasiparticles in the three samples become Cooper pairs;

(ii). The overlap of the curves of resistance versus temperature of the film and the wire I in the Fig. 2 indicates that the COI might do not appear;

(iii). For the wire II, Fig. 2 shows: The COI state and MIT appear at $T < T_{Curie} = 145$ K and at $T_p = 91$ K, respectively. This fact indicates that the COI might appear, and the COI can disappear at low temperature;

(iv). Both Figs. 3a and 4a show that in strong electric field the resistance reduces. This fact shows that the electric field can reduce the hight of barrier two FMM domains, mediated by COI region.

(13). $(La_{(1-x)/2}Sr_{(1+x)/2})_{2n}Mn_nO_{3n+1}$ with n=1 and x= 0.0 - 0.7 never

has CMR [15] , although the so-called K_2NiF_4 structure in case of the high-Tc cuprates $(La_{(1-x)/2}Sr_{(1+x)/2})_{2n}Cu_nO_{3n+1}$ with n=1 and x= 0.05 - 0.3 has Cooper pairs [11].

Explanation: Experiments tell us that $La_{(1-x)}Sr_{(1+x)}MnO_4$ has no magnetic phase [15], while $La_{(1-x)}Sr_{(1+x)}CuO_4$ has AF magnetic phase [11]. Therefore, the former and the later do not and do have pairing potential, respectively.

(14). The page 47 in Ref. [12] wrote: "Metal-Insulator transition is not absolutely necessary condition for the appearance of CMR. This is for instance the case of the manganite $Pr_{0.7}Ca_{0.26}Sr_{0.26}MnO_3$, that exhibits a semiconducting behavior in a zero magnetic field, and is transformed into a ferromagnetic metal when submitted to a magnetic field 5 T (Fig. 3), so that a resistance ration of 10^{11} can be reached at 30 K for this compound."

Explanation: The appearance of CMR depends only on the appearance of Cooper pairs in FM metal state.

(15). The page 47 in Ref. [12] wrote: "In order to explain the particular transport and magnetic properties of manganese perovskites, two parameters have to be taken into consideration, the hole carrier density and the overlapping of the manganese and oxygen orbitals. Such an approach is common to all oxides and has previously been applied in the high-T_c superconducting cuprates."

Explanation: In the formula of pairing potential, TLSMI, there is Kondo coupling constant J_K, which depends on the hopping integral between orbitals of 3d of manganese and 2p of oxygen. The size of the hopping integral depends on this overlapping. The hole carrier density has to be considered because the Cooper pair is the pairing of two holes other than the 3d electron of Mn atom.

15

(16). Ref. [12] pointed out: "The systematic study of the substitution of various M elements for Mn in the CMR perovskite $Pr_{0.7}Ca_{0.2}Sr_{0.1}MnO_3$ has been performed for M=Al, Ga, In, Ti. It shows that whatever the element, the transition temperature T_c (or T_{max}) from the FMM to PMI state decreases dramatically as the content of the doping element increases. This is illustrated by the R(T) curves of the series $Pr_{0.7}Ca_{0.2}Sr_{0.1}Mn_{1-x}Al_xO_3$ (Fig. 26), where it can be seen that T_{max} is decreased by about 12 K per percent of Al atom introduced on the Mn site. The corresponding magnetoresistance is in fact correlated to T_{max}: it increases significantly as x increases. $R_{H=0}/R_{H=7T}$ reaching 10^3 at 71 K for 6% Al per Mn.

Explanation: The pairing potential TLSMI depends on the interaction between $O_{2p\sigma}$ carrier and the local spin of Mn ion. The substitution reduces TLSMI, and thus leads to the number of Cooper pairs decreases.

(17). In page 115-116 of Ref. [12] there were reports on CMR in $R_{2/3}Ca_{1/3}MnO_3$ compounds: "In this series of compounds $M^{+4}/M^{+3} = 1/2$, R=La-Y, Pr, and La-Tb. The change of the rare-earth ion produces a distortion of the perovskite structure in the following three ways: the smaller the ions, the smaller the Mn-O-Mn bond angle. This fact brings about a narrowing of the e_g electronic bandwidth and, consequently, the double-exchange interaction is weakened." In case of $R = La_{0.6}Y_{0.07}$, at 160 K insulator-metal transition occurs and, simultaneously, a paraferromagnetic transition takes place. The drastic decrease of T_{Curie} at zero magnetic field from 210 K for $R = La_{0.67}Y_0$ (See page 98 of Ref. [12]) to 160 K for $R = La_{0.6}Y_{0.07}$.

Explanation: This experiment is explained in terms of the narrowing of the e_g band as a consequence of the lattice distortion produced by the substitution of La by a smaller ion Y [12]. This paper will give a little different explanation from our theory of formation of Cooper pairs. The narrowing of the e_g band

16

comes from the smaller Mn-O-Mn bond angle, which leads to the weakening DE interaction, and FM, and further leads to stronger FM, and TLSMI, which leads to the formation of free but random Cooper pairs.

(18). In page 116 of Ref. [12] there is: "The residual magnetoresistance at low temperature is due to the contribution from the tunneling through the grain boundaries. An additional contribution in this compound in the FM phase can be attributed to the noncollinear alignment of the magnetic moments below T_{Curie} even at the lowest temperature."

Explanation: Due to that the large residual magnetiresistances can exist even at single crystal and epitaxial film, the contribution from the tunneling through the grain boundaries is not necessary to consider. This paper thinks the an additional contribution in this compound in the FM phase can be attributed to breaking of Cooper pairs and random motion.

(19). $Pr_{2/3}Ca_{1/3}MnO_3$ at $4 < T < 210$ K is in COI state. A first-order insulator-metal transition can be induced by magnetic field. Below $T_N = 150$ K this compound orders antiferromagnetically in the CE-type structure. Below 100 K a canting of the magnetic moment takes place giving to a AM component. Much effort was devoted to establish the tight connection between the magnetic andtransport properties in this compound (See the page 120 of Ref. [12]) For example, at 12 T the field-induced transition from COI state to FM metal state is shifted to $T_{CO} = 210$ K from $T_{CO} = 80$ at 6T. It seems that at this value of field, the CO is completely suppressed in the whole temperature range. These results can be understood considering that the volume distortion associated with the charge localization disappear as the charge is released. When the whole charge is released, the thermal expansion recovers the Grüneisen thermal dependence due to the phonon contribution, which is the situation of the metallic state in $Pr_{2/3}Ca_{1/3}MnO_3$. There are

17

two problems: (i). Why the magnetic field can suppress CO in the whole temperature range (ii). What appears after suppressing CO?

Explanation: (i). The strong magnetic field causes the enhancement of FM, and thus the enhancement of paring potential, TLSMI. The later leads to formation of Cooper pairs at 210 K and 12 T. Of course, when the temperature goes down, more and more Cooper pairs appear. (ii). Cooper pairs is the origin of CMR.

(20). For $(La_{1-x}Tb_x)_{2/3}Ca_{1/3}MnO_3$ the FM state is always related to a metallic state and the PM, AFM, and spin-glass states to an insulating behaviour (See page 133 of Ref. [12].). For $(La_{0.67}Tb_{0.33})_{2/3}Ca_{1/3}MnO_3$ the sample is in SGI state (See the Fig. 46 in page 135 of Ref. [13].). At fields higher than 5 T the resistivity is low enough to be measured with our experimental set-up at low temperature. The role of the magnetic field is to align the spin-glass clusters and to increase their size to produce the percolation, which leads to the reduction of the resistivity.

Explanation: The role of the magnetic field is to align the spin-glass clusters and to enhance the FM in every spin-glass clusters, which leads to stronger pairing potential, TLSMI. The appearance of more Cooper pairs leads, of course, to the reduction of resistivity. The so-called "to increase their size to produce the percolation" is only a guess, not reliable, at least, at present stage, and is not necessary.

(21). One of the problem of manganese perovskites is the non-stoichiometry of the oxygen, which gives rise to a drastic modification of the structural, magnetic and magnetotransport propeties. An oxygen excess can not be accommodated in this structure (See page 136 of Ref. [13].).

Explanation: Oxygen vacancy leads to the change of number of $O_{2p\sigma}$ hole carriers, and thus leads to variation of transport properties. Oxygen vacancy

leads also to reduces the DE interaction, which gives rise to reduce FM, which gives rise to reduce TLSMI.

(22). The Mn and La vacancies in equal amount are produced. The real formula is $(La_{3/(3+\delta)}Mn_{3/(3+\delta)}O_3$ (δ=0, 0.025, 0.07, 0.1, 0.15). In this compounds the Mn^{+4} concentration is $\%Mn^{+4}$=200×δ. For this materials three groups gave different observation: (i). MI transition occurs for $\delta \geq 0.15$; (ii). The resistivity always shows an insulator behaviour; (iii). The resistivity always shows an insulator behaviour and only at $\delta = 0.15$ magnetoresistance at 12 T is observed (See page 136 of Ref. [12].).

Explanation: Why CMR is observed at $\delta = 0.15$? A possible explanation is as follows. page 146 in Ref. [12] gives the following data: the magnetic moment of the Mn ion are $\mu(\mu_B)$=3.49, 2.92, 3.26, 2.86, and 0.78 for $delta$=0, 0.025, 0.07, 0.1, and 0.15, respectively. Due to the smallest moment of Mn ion of $\delta = 0.15$ when the magnetic field is applied, the relative variation of the moment of Mn ion is larger, which gives rise to the larger relative enhancement of FM. In this case the pairing potential has a larger relative increase. The appearance of Cooper pairs gives rise to the reduction of resistivity.

(23). For ferromagnetic, metallic state of the optimally doped $(La_{1-x}(Sr, Ca)_x MnO_3$ ($x \approx 0.33$), in high quality single crystals as well as thin films, the resistivity increase is very rapidly with temperature, and can be fitted to the dependence (See page 330 of Ref. [12].).

$$\rho(T) = \rho_0 + AT^2 + BT^{9/2}.$$

Explanation: Although Ref. [12] gave an explanation, we still like to propose our explanation. We think that both CMR in samples $(La_{1.2}Sr_{1.8}Mn_2O_7$ in Fig.3 and $(La_{1-x}(Sr, Ca)_x MnO_3$ ($x \approx 0.33$) are caused by Cooper pairs.

(24). Ramakrishnan pointed out in the pages 325 of Ref. [12] that: "The

ferromagnetic, metallic state of the optimally doped $(La_{1-x}(Sr, Ca)_x MnO_3$
$(x \approx 0.33)$, in high quality single crystals as well as thin films, has a residual
resistivity as small as 100 $\mu\Omega$cm, corresponding to a mean free path of order
40 to 60 Å, which is ten or more than the maximum metallic resistivity value
of 1 to 2 mΩcm. However, many polycrystalline systems with nearly optimum
size of the rare earth (or substituent) ions as well as systems with non optimal
(generally smaller) ion size show extremely high values of residual resistivity.
These values can be several orders of magnitude higher than the maximum
metallic resistivity, and yet the resistivity seems to flatten out at $T \to 0$"
without increasing to infinity as it should for a insulator. This is in contrast
to the behaviour of all other strong disordered and correlated systems in
which as a function of disorder or correlation, a maximum metallic resistivity
(the Mott value corresponding to $k_F l$ 1) separates the disordered metal from
the insulator.

An example of the spectacular violation of the Mott limit is the resistivity
of $Re_{0.7}A_{0.3}MnO_3$ films, where the Lanthanide Re is either Nd or La, and
the alkaline earth ion A is either Sr or Ba. The $Nd_{0.7}Sr_{0.3}MnO_3$ sample
has a residual resistivity of 10^4 Ωcm, and a FM temperature T_c of about 100
K, while $La_{0.7}Sr_{0.3}MnO_3$ sample has a residual resistivity of 10^{-4} Ωcm, and
$T_c = 300$ K. The two systems have the same hole carrier density. The main
difference of the two systems is: "Nd^{3+} is much smaller that La^{3+}. We note
that the residual resistivity at $< r_A >= 1.12$ Å can be as much as 10^6 times
larger than the maximum metallic value at $< r_A >= 1.20$ Å! (See the Fig.
4. in Ref. [12].)" Ramakrishnan pointed out in the pages 335 of Ref. [12]
that: "The reduction in the mean rare earth ionic radius is accompanied by a
bending of the Mn-O-Mn bond, from 170○ to 155° as r_A decreases from 1.20
to 1.12 Å."

Explanation: The bending of the Mn-O-Mn bond, from 170∘ to 155°
as r_A decreases from 1.20 to 1.12 $\AA$ leads to reduction of value of T_c from
300 K to 100 K, which means FM reduction. The later gives rise to the
weakening Cooper pair potential, and thus to the value of voltage of Cooper
pair breaking. In many measurements of resistivity the applied voltage is
about 100 meV. An very rough estimation is: The breaking voltage about 1
meV and 0.1 meV for $< r_A >= 1.2 \AA$ and $1.12 \AA$. Therefore, the free flight
time of Cooper pairs in system with $< r_A >= 1.2 \AA$ is much larger than tha
of system with $< r_A = 1.12 \AA$.

(25). Sun and Dessau published a paper in Nature Physics in 2007 [20].
This paper discovered: "The temperature induced transition from a metallic
to an insulating state in a solid is generally connected to a vanishing of the
low-energy electronic excitations. Here we show the first direct evidence of a
counter-example, in which a significant electronic density of states at the Fer-
mi energy exists in the insulating regime. In particular, angle-resolved pho-
toemission data from the colossal magnetoresistive oxide $La_{1.24}Sr_{1.76}Mn_2O_7$
show clear Fermi-edge steps, both below the metalCinsulator transition tem-
perature T_c, when the sample is globally metallic, and above T_c, when it is
globally insulating. Further, small amounts of metallic spectral weight sur-
vive up to temperatures more than twice T_c. Such behaviour may also have
close ties to a variety of exotic phenomena in correlated electron systems,
including the pseudogap temperature in underdoped cuprates." "T^* signals
the emergence of the metallic domains, which become long range at T_c. ...
the intercepts should reach zero near 300 K, which should roughly be the
temperature where the first bits of metallic weight become apparent. We call
this temperature T^*.

Explanation: The Fig. 1 of this paper has proved that for the CMR

manganite of Ref. [3] the pseudogap can exist at temperature much higher than $T_c = 245$ K, which means that the electronic density of states at the Fermi energy exists in the insulating regime. The so-called 'metallic domains' are matallic FM domains. The so-called 'the first bits of metallic weight' are the first bits of FM metallic weight. From Figs. 1, 2, and 3 we deduce that when the FM metallic domains appear, these domains are of CMR, Cooper pairs, and pseudogap. Therefore, the so-called 'T^*' is the beginning temperature to appear the pseudogap.

(26). Dagotto proposed in 2005 in Ref. [8] the following unsolved problem: "The existence of the predicted new temperature scale T^* above the Curie temperature ($\approx$ M-I transition tempetatuire) should be further investigated. (i) Thermal expansion, magnetic susceptibility, x-rays, neutron scattering and other techniques have already provided results supporting the existence of a new scale T^*, where clusters start forming upon cooling. In fact, very early in manganite investigations, the group of Ibarra at Zaragoza reported the existence of such a scale, in agreement with more recent theoretical and experimental developments. Recent results also report the existence of T^*, using electron spin resonance and magnetic susceptibility measurements. This scale should manifest itself even in the dc resistivity, as it does in the high-temperature superconductors at the analogue T^* pseudogap temperature. (ii) In addition, the specific heat should systematically show the existence of structure at T^* due to the development of short-range order (at T^*, even a glassy phase transition may occur, as recently proposed). (iii) The dependence of T^* with doping and tolerance factors should be analysed systematically. Theoretical studies suggest that the tolerance factor may not change T^* substantially, although it affects the ordering temperatures significantly. Is there experimental support for this prediction? (iv) Is the crude

22

picture of the state between T_c and T^* shown in figure 4 qualitatively correct?"

Explanation: The so-called 'new temperature scale T^{*}' in Ref. [8] is the temperature of appearance of pseudogap. The T^* in CMR manganites and high-T_c cuprates is exactly same thing.

(27). Dagotto proposed in 2005 in Ref. [8] the following unsolved problem: "Temperature dependence of the dc resistivity of manganites has not been sufficiently analysed. Can non-Fermi-liquid (NFL) behaviour be shown to be present in metallic manganites, as it occurs in many other exotic metals?

Explanation: It is not necessary to explain CMR in terms of non-Fermi-liquid (NFL) behaviour. The Fermi surface nesting is necessary for CMR and pseudogap.

(28). Dagotto proposed in 2005 in Ref. [8] proposed an unsolved theoretical issue: "Can a rough temperature dependence of the dc resistivity be calculated within the percolative scenario? We do have resistor-network calculations that match the experiments, but not a simple anybody-can-use formula. This is a complicated task due to the difficulty in handling inhomogeneities."

Explanation: Our numerical calculation for dependence of CMR on temperature in Fig. 3 clearly indicates that the so-called "resistor-network calculations" is not necessary.

(29). Dagotto proposed in 2005 in Ref. [8] proposed an unsolved theoretical issue: "For the explanation of CMR, is there a fundamental difference between JT- and CoulombC based theories? Technically, it is quite hard to handle models where simultaneously the CoulombCHubbard interactions as well as the electronCphonon couplings are large. However, so far, for CMR phenomena, the origin (JT versus Coulomb) of the competing phases does

23

not appear to be crucial, but only the competition itself is. Is this correct?

Explanation: Both JT and Coulomb are not decisive for CMR.

(30). Although the value of the pseudogap in CMR manganites is much larger than that in the high-T_c cuprates, CMR manganites have not macroscopic superconductivity.

Explanation: Ref. [11] proves that the condition of emergence of macroscopic superconductivity is that Josephson coupling energy $E_J(T)$ between Cooper pairs is large enough and [11]

$$E_J(T) \propto \frac{\Delta(T)}{R_n}. \qquad (4.2)$$

For manganites, the resistivity without the Cooper pairs, $\rho_{n,manganites}$, is nearly equal to $100 \times \rho_n$, where ρ_n is the resistivity of high-T_c cuprates in normal state. Although the pseudogap $\Delta_{manganites}$ is nearly equal to $10 \times \Delta_{cuprates}$, due to small $E_J(T)$ the maganites never have macroscopic superconductivity. Along this line, it is not impossible that in future one will discovery room temperature macroscopic superconductivity by making a magnetic material with large pseudogap but small resistivity at room temperature.

5. Conclusions on the origin of pseudogap and CMR

From the fifteen similarities in electronic, lattice, and Hamiltonian structures of CMR manganites with the high-T_c cuprates, we infer that the pseudogaps and CMR of manganites are caused by the formation of Cooper pairs. This inference on Cooper pair's existence in CMR manganites are further verified by the uniform and quantitative explanations for the thirty six experimental facts about the pseudogap and CMR. Therefore, this paper concludes: (1). The observed d- and p-wave symmetry pseudogaps in FM and AFM regions,

respectively, of CMR manganites come from Cooper pairs; (2). The Cooper pair consists of two oxygen $2p\sigma$ holes, and exists in the MnO_2 plane; (3). The motion of Cooper pairs is random but free; (4). CMR is caused by the free motion of Cooper pairs; (5). The new Hamitonian in Eq. (2.1)′ should become a starting point of theoretical study on CMR manganites. One should abandon many Hamiltonians to describe CMR manganites, proposed before this paper, for example in Ref. [9].

6. Six properties of Cooper pairs in CMR manganites

Sections 2, 3, 4, and 5 show that the properties of Cooper pairs in CMR manganites are same as that of the Cooper pairs in the pseudogap state of the high-T_c cuprates at $T_c < T < T^*$.

(i). The free motion has critical velocity, which is given y the Landau criterion [6,11]

$$v_c = \frac{\Delta}{\hbar k_F},\qquad(6.1)$$

where Δ, $\hbar$, and k_F are pseudogap, Planck constant, and Fermi wavenumber, respectively.

(ii). The motion satisfies Newton equation, if velocity of Cooper pair is less than v_c;

(iii). Do not have Meissner effect, and thus have body current other than surface current [24];

(iv). In the MnO_2 plane, Carriers = Cooper pairs + single particles;

(v). The motion of Cooper pairs does not produce Joule heat;

(vi). For FM, field enhances Cooper pairing potential TLSMI.

7. Applications of CMR manganites

The exact and general definitiion of pseudogap is: The pseudogap is a true energy gap above Fermi surface. We call generally any body with pseudogap pseudogapbody. Many applications of the high-T_c cuprates and pseudogapbody have been given in Refs. [6,11,23,22]. Many CMR manganites have the pseudogap at room temperature. Usuing the six properties in section 6, we find that CMR manganites have many possible applications

7.1. Applications in energy
7.1.1. Permanent current and permanent strong magnet

A permanent current in a ring made by $La_{0.625}Ca_{0.375}MnO_3$ can be induced by the change of magnetic flux in the ring at room temperature [23,25,26,6]. For example, set the radius of the ring is 0.5 m, and the radius of rings wire is 3 mm. The induction critical current in this ring is $I_c = 2.94 \times 10^8$ A, the inductance is $L = 3.37 \times 10^{-6}$ H, $B_{maximum} = LI_c/(\pi 0.5^2) = 1279$ T in the opening of the ring, the maximum magnetic pressure between the two such rings and at very small distance is $P_{mag-pre} = 6.36 \times 10^{10}$ Pa, and, thus, the maximum magnetic levitation is 5.2×10^9 kg, and so big value of $B_{maximum}$ can storage energy $4.0 \times^{11}$ J/m^3. If we use the high-T_c cuprates to make the same size ring working at 77 K, then the supercurrent is in the ring's surface with thickness 100 nm due to Meissner effect [25], and, thus $I_c = 1.96 \times 10^3 << 2.94 \times 10^8$ A. If the high-T_c cuprates are hard superconductors, then $I_c = 1.96 \times 10^5$ A. It is important to note that in magnetic field the d-wave superconductivity of the high-T_c cuprates and the p-wave superconductivity of CMR manganites are weakened and enhanced, respectively. Thus, the superconductivity in conventional superconductors and the high-T_c cuprates is very much weakened by magnetic field [27]. For

the energy storage of conventional superconductors and the high-T_c cuprates can see Ref. [28].

7.1.2. Power transmission

It is well known that the resistivity of wire made by $La_{0.625}Ca_{0.375}MnO_3$ is [3]

$$\rho(300K) = 1.4 \times 10^{-3}\Omega cm. \tag{7.1}$$

Let us calculate that due to free motion of Cooper pairs, the effective resistivity at 300 K.

(i). $v_c = 2.06 \times 10^6$ cm/second. Thus, critical kinetic energy $E_{critical} = 2.3$ meV.

(ii). We apply voltage on the two ends of a transmission wire $U_{applied} = 2.3$ mV. $U_{applied}$ will accelerate Cooper pairs in the transmission wire. Average velocity of these Cooper pairs $v_{average} = v_c/2$. Thus, average current density $J_{average} = J_c/2$.

At last, we have

$$\rho_{effective}(300K) = \frac{U_{applied}}{J_{average} \times Length}. \tag{7.2}$$

If $length = 1\ km = 10^5$ cm, $\rho_{effective}(300K) = 4.6 \times 10^{-17}\Omega$ cm.

Besides a little, due to that the applied voltage is used just for acceleration of Cooper pairs, there are no any generation of Joule heat.

There is a sharp question that why all measurements from 1950 to 2014 indicate: manganites are high resistance materials? For example, for $La_{0.625}Ca_{0.375}MnO_3$, $\rho(300K) = 14 \times 10^{-3}\Omega$ cm$>> \rho_{effective}(300K) = 4.6 \times 10^{-17}\Omega$ cm.

Actually, the answer is very simple. Now available four point probes to measure resistivity give following standard data for a wafer of thickness 500 nm, made by $La_{0.625}Ca_{0.375}MnO_3$: At first, the constant current is $I = 4.5$

mA; Then, the voltage is $V = 68$ mV; We obtain $\rho(300K) = 4.53 \times t \times I/V = 14 \times 10^{-3} \Omega$ cm. We know that the critical voltage, i. e., breaking voltage of Cooper pairs, is less than 2.3 mV. Therefore, the Cooper pairs are definitely broken many times in the wafer. So, we get always high resistivity for manganites. Therefore, we have to modify the four point probes.

For example, we design the following "small and constant voltage method". Assume that our sample is made by $La_{0.625}Ca_{0.375}MnO_3$, length=2 cm, thickness t=100 μm, wide=1 cm. At first, we apply constant (!!!) voltage U=2.3 mV, then from Eq. (7.2) $\rho_{effective}(300K) = 2.3 \times 10^{-12} \Omega$ cm$<< 14 \times 10^{-3} \Omega$ cm.

7.1.3. Passive microwave circuits

Principle of applications: In alternating field the current is carried by both Cooper pairs and normal carriers, and only about 10^{-8} of the total current is carried by the normal carriers, and there is only a minute dissipation of power [26].

For example, the quality factor of resonator, Q=Uf/P, where U=total energy stored in the oscillator, f=frequency of resonance, P=power dissipation in one circle. $Q_{CMR-manganite} = 10^{11}$. $Q_{Copper} = 10^4$ at 10 GHz [26].

Passive microwave circuits are: resonator, microwave transmission line, filters, frequency agile devices, antenna, delay lines [26].

7.2. Applications in electronic device
7.2.1. Light-emitting devices (generator, mixer, ...)

Principle of light-emission by Josephson tunneling junction: In Fig. 4 the left Cooper electron pair tunnels to the right, obtains energy 2$|e|$V due to its free motion. This process is energy-nonconservative. To keep energy conservation

this Cooper pair emits one photon with energy $\hbar\nu = 2|e|$V, and returns to the left [11,6].

Therefore, using, for example, $La_{0.625}Ca_{0.375}MnO_3$ to make Manganite-Insulator-Manganite tunneling junction, one can easily obtain photons from very long wavelength to visible light at 300 K by just changing the voltage applied. Actually, many kinds of weak connections have this effect as well [11].

7.2.2. Light-detecting devices

Principle of light-detect by CMR manganites: One Cooper pair absorbs one photon with energy $> 2 \times 250$ meV (for $La_{0.625}Ca_{0.375}MnO_3$), breaks, and becomes two quasiparticles other than just one quasiparticle in case of semiconductor. Therefore, the sensitivity of light-detector of CMR manganites is higher than that of semiconductors.

7.2.3. Schottky barrier solar cell

Principle of Schottky solar cell: Incident photons produce carriers in semiconductor or CMR manganites, these carriers will move due to Schottky barrier between metal and semiconductor or CMR manganite.

Set $\eta = conversion\ efficiency\ of\ light\ to\ electricity$. For example, band gap of n-Si=1.12 eV. Pseudogap of $La_{0.625}Ca_{0.375}MnO_3$=0.25 eV. There are three reasons that $\eta_{n-Si} << \eta_{LCMO}$.

(i). Semiconductor and $La_{0.625}Ca_{0.375}MnO_3$ absorb one photon produce one and two quasiparticles, respectively. This factor demands $\eta_{n-Si} = 0.5\eta_{LCMO}$;

(ii). Due to the difference of scale of gap, n-Si and $La_{0.625}Ca_{0.375}MnO_3$ absorb $\approx$3/4 and $\approx$4/4 of solar spectrum, respectively;

(iii). $\eta \propto Light-absorbing\ coefficient\ G \propto (E = E_g)^{1/2}$. For $La_{0.625}Ca_{0.375}MnO_3$

$E_g = 0.5$ eV. For n-Si $E_g = 1.12$ eV. A rough estimation gives:

$$\frac{G_{La_{0.625}Ca_{0.375}MnO_3}}{G_{n-Si}} = \frac{(2-0.5)^{1/2}}{(2-1.12)^{1/2}} = 1.305. \tag{7.3}$$

Now, the best expectation value of η_{n-Si} is 25%. Thus, from (i), (ii), and (iii),

$$\eta_{LCMO} = 25\% \times 2 \times \frac{1.305}{0.75} = 87\%. \tag{7.4}$$

8. Summary on applications of CMR manganites

From the discussions in section 7 we can see the advantages of CMR manganites over semiconductors and superconductors. Tables 2 and 3 give the detail comparisons.

From Table 2 and 3 we can see that the applications of CMR manganites will initiate a new times of material science and material engineering.

New times=

=Times of microscopic superconductivity

=Times of Cooper pairs

=Times of pseudogapbody

≈Times of CMR manganites

=90% and 80% in applications of superconductors and semiconductors,

will be substituted by CMR manganites, respectively, in future 30 years.

Main reasons for the last equality are:

Superconductors need to work, at lest at present, at 77 K, while CMR manganites can work at 300 K;

Superconductors have surface current, while CMR manganites have body current; Due to this reason, even the macroscopic superconductivity at room tempersature is discovered in future, CMR manganites have still advantages

in many applications.

Semiconductor devices produce Joule heat, while CMR manganites do not.

Acknowledgement

References

[1] D. S. Dessau *et al.*, Phys. Rev. Lett. 81 (1998) 192.

[2] N. Mannella *et al.*, Nature, 438 (2005) 474.

[3] U. R. Singh *et al.*, J. Phys.: Condens. Matter, 21 (2009) 355001.

[4] J. Kim *et al.*, Phys. Rev. Lett. 110 (2013) 217203. arxiv.org/pdf/1303.0244.

[5] F. Massee *et al.*, Nature Physics, 7 (2011) 978.

[6] Fu-sui Liu, *Advanced Quantum Mechanics upon Theotems*, (Nova, New Yourk, February 2014).

[7] Y.D. Chuang and D.S. Dessau, in *The Electronic Structure, Fermi Surface, and Pseudogap in Manganites*, Ed, T. Chatterji, (Kluwer academic publishers, Dordrecht, 2004), pp. 93-129.

[8] E. Dagotto, New J. Phys. 7 (2005) 67.

[9] E. Dagotto, *Nanoscale Phase Separation and Colossal MagnetoResistance*, (Springer, Berlin, 2003), p. 118, 81, 15, 16, 122, 86, 27, 335, 46, 47, 315, 84, 74, 21, 17.

[10] D. F. Dionne, *Magnetic Oxides*, (Spronger, Berlin, 2009), p. 98.

[11] Fu-sui Liu, *Genaral Theory of Superconductivity*, (Nova, New York, 2008), p. 95, 111, 163.

[12] C. N. R. Rao and B. Raveau, *Colossal Magnetoresistance, Charge Ordering and Related Properties of Manganese Oxide*, (World Scientific, Singapore, 1998), p. 281, 340, 207, 194, 47, 71.

[13] C. Sen*et al.*, Phys. Rev. Lett. 105 (2012) 097203.

[14] Y. Moritomo, A. Asamitsu, H. Kuwahara, Y. Tokura, Nature, 380 (1996) 380

[15] Y. Tokura, "Colossal Magnetoresistive Oxides", (Gordon and Breach Publishers, New York, 2000), p. 149, 45, 18, 89.

[16] C. H. Shen and R. S. Liu, Journal of Appl. Phys. 86 (1999) 2178.

[17] Zhiqiang Chen, "Probing spin, chage, and lattice coupling in manganites". PhD thesis, New Jersey Institute of Technology, USA, 2008, 7, 92-95.

[18] Haifen Li, "Synthesis of CMR manganites and ordering phenomena in complex transition metal oxides". PhD thesis, Rheinisch-Westf?lischen Technischen Hochschule Aachen, Germany, 2008, 18.

[19] Li-Min Cai, et al., Chin. Phys. B, 23 (2014) 097103.

[20] Z. Sun, D. S. Dessau, et al., Nature Physics, 3 (2007) 284.

[21] Phys. Rev. Lett. 108 (2012) 016403. arXiv:1105.5468v3 [cond-mat.str-el] 1 Apr. 2012.

[22] H. Matsukawa and H. Fukuyama, J. Phys. Soc. Jpn. 58 (1989) 2845.

[23] H.-B. Yang1, J. D. Rameau1, P. D. Johnson1, T. Valla1, A. Tsvelik1, G. D. Gu1, Nature, 456 (2008) 77.

[24] Fei Tan and Fu-sui Liu, J. Superconductivity and novel magnetism, 25, (2012) 299.

[25] Fu-sui Liu, Journal of Superconductivity and novel magnetism, 25 (2012) 215.

[26] The page 147 in Ref. [6] concluded that the Cooper pairs in the pseudo-gap state does have Meissner effect. This conclusion is wrong, because one cannot deduce from common velocity that there is common phase of the Cooper pairs in the pseudogap state.

[27] W. Bukel and R. Kleiner, *Superconductivity*, (Wiley-VCH, Tubingen, 2004), p. 12.

[28] P. J. Lee, *Engineering of Superconductivity*, (John Wiley & Sons, New York, 2001).

[29] Zhaoshun Gao, Yanwei Ma et al., Scientific Reports, 2 (2012) 998. DOI: 10.1038/srep00998.

[30] P. Tixador, *Superconducting magnetic energy storage*, in *High Temper-arure Superconductors (HTS) for Energy Applications*, Ed. by Ziad Mel-hem, (Woodhead Publishing, Cambridge, 2012), p. 294.

[31] Xinwei Zhang, et al., *Studies on High Temperature Superconductivity*, (Sichuan Education, Chengdu, 1989), p. 389.

Table 1: The fifteen similarities between CMR manganites and high-T_c cuprates in aspects of lattice, electronic, and Hamiltonian structures

High-T_c cuprates		CMR manganites
Perovskite type-like structure	1	Perovskite type-like structure
CuO_2 plane	2	MnO_2 plane
In CuO_2 plane, lattice constant (O-O distance) ≈ 0.39 Å	3	In MnO_2 plane, lattice constant (O-O distance) ≈ 0.39 Å
CuO_2 plane has local spin of Cu ions	4	MnO_2 plane has local spin of Mn ions
Carriers are $O_{p\sigma}$ holes	5	Carriers are $O_{p\sigma}$ holes
$O_{p\sigma}$ holes are in CuO_2 plane	6	$O_{p\sigma}$ holes are in MnO_2 plane
Nesting Fermi surface in CuO_2 plane	7	Nesting Fermi surface in MnO_2 plane
Strong correlation Hamiltonian in CuO_2 plane is in Eqs. (2.1) and (2.1)'	8	Strong correlation Hamiltonian in MnO_2 plane is in Eqs. (2.1) and (2.1)'
Kondo Hamiltonian between hole and local spin $\propto J_K$	9	Kondo Hamiltonian between hole and local spin $\propto J_K$
Heisenberg Hamiltonian between local spins $\propto J$	10	Heisenberg Hamiltonian between local spins $\propto J$
Two local spin-mediated interaction (TLSMI) in CuO_2 plane	11	Two local spin-mediated interaction (TLSMI) in MnO_2 plane
Formula of TLSMI in Eq. (2.2)	12	Formula of TLSMI in Eq. (2.2)
Pseudogap $T_c < T < T^*$	13	Pseudogap $0 < T < T^*$
3d and 2p orbitals are important	14	3d and 2p orbitals are important
Values of J_K, J, ...	15	Values of J_K, J, ... are nearly same as that of high-T_c cuprates

Caption of Fig. 3: Diagram of resistivity versus temperature. The data curves for $La_{1.2}Sr_{1.8}Mn_2O_7$ are adapted from Refs. [14,15]. The circles and triangles are our numerical results for 0 and 5 T, respectively. Field is parallel to MnO_2 plane. ρ_{ab} and ρ_c are the inplane and interplane resistivity.

Table 2: The contrasts of CMR manganites with semiconductors

Semiconductors		CMR manganites
6 weakness		6 advantages
Produce Joule heat	1	not produce Joule heat
Low number density ($\approx 10^{16}/cm^3$)	2	High number density ($\approx 10^{21}/cm^3$)
Absorb one photon, produce one carrier	3	Absorb one photon, produce two carriers
No Josephson effrect	4	Josephson effect
Not easy to get small band gap	5	Easy to get small band gap
Best transformation time $\tau = 10^{-13}$ S	6	Best transformation time $\tau = 10^{-15}$ S [30]
1 advantage		1 weakness
Can have large band gap, such as 4.9 eV for $\beta - Ga_2O_3$	1	At present, cannot have large gap, such as the biggest pseudogap$\leq$1 eV

Table 3: The contrasts of CMR manganites with superconductors

| Superconductors		CMR manganites
5 weakness		5 advantages
Cannot work at 300 K	1	Can work at 300 K
Surface current	2	Body current
Field reduces current density	3	Field enhances current density
Cannot have large pseudogap at 300 K	4	Can have large pseudogap at 300 K
The smallest transformation time $\tau = 1 \times 10^{-14}$ second	5	The smallest transformation time $\tau = 1 \times 10^{-15}$ second [30]
1 advantage		1 weakness
Josephson effect in magnetic field	1	No Josephson effect in magnetic field
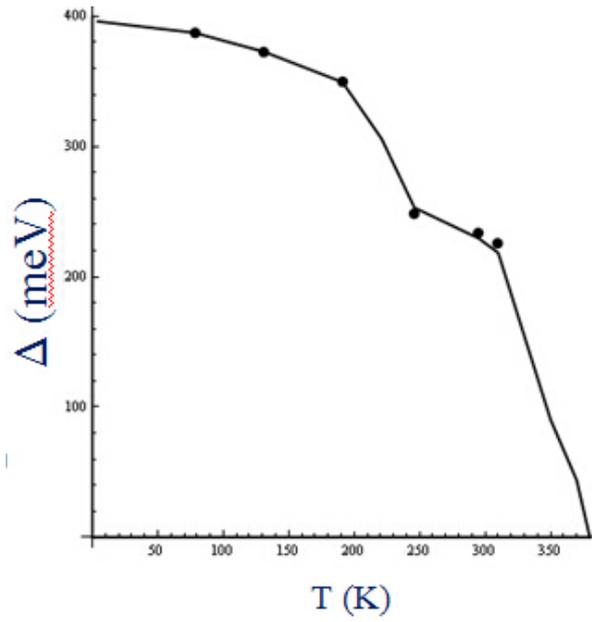
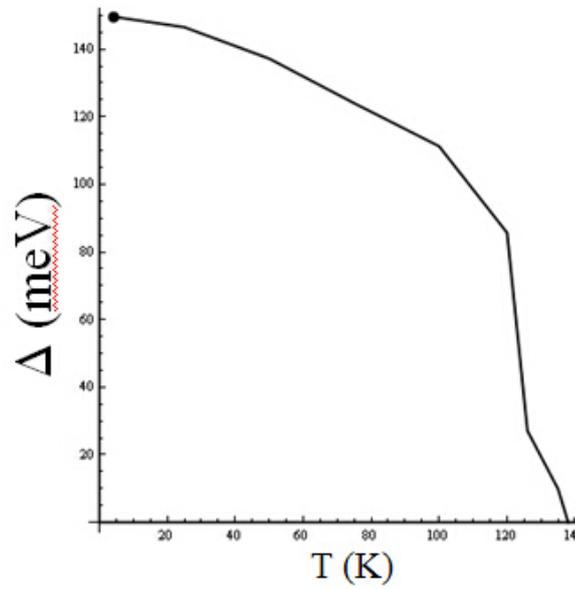Figure 1: Diagram of pseudogap Δ (meV) versus temperature T (K) for $La_{0.625}Ca_{0.375}MnO_3$. The data come from Ref. [3].

Figure 2: Diagram of pseudogap Δ (meV) versus temperature T (K) for $La_{1.2}Sr_{1.8}Mn_2O_7$. The data come from Ref. [5].
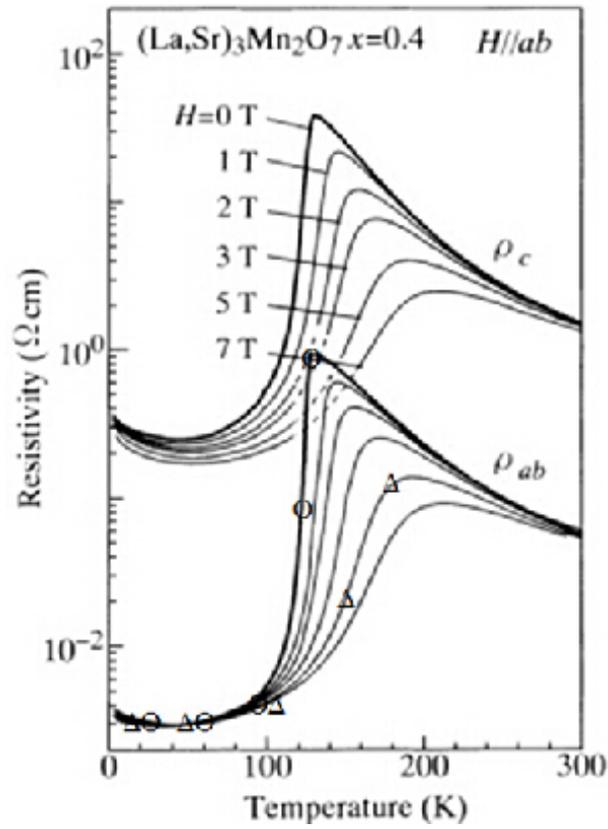
36

Figure 3: Diagram of resistivity versus temperature. The data curves for
La_1 ̶ ̶ ̶
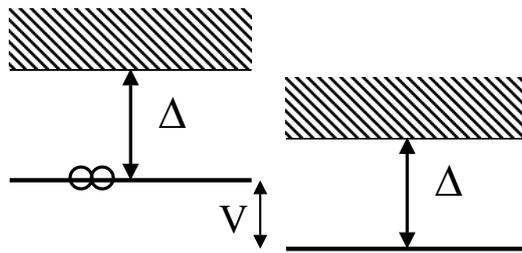are
plar

Figure 4: Diagram of energy level of Josephson junction (Adapted from Ref.
[1 1].). (The applied Voltage V $\leq$ breakdown voltage of the junction $\approx 1 - 2$
eV [11].)